Measurements of higher alkanes using NO^+ chemical ionization in PTR-ToF-MS: important contributions of higher alkanes to secondary organic aerosols in China

Chaomin Wang[1,2], Caihong Wu[1,2], Sihang Wang[1,2], Jipeng Qi[1,2], Baolin Wang[3], Zelong Wang[1,2], Weiwei Hu[4], Wei Chen[4], Chenshuo Ye[5], Wenjie Wang[5], Yele Sun[6], Chen Wang[3], Shan Huang[1,2], Wei Song[4], Xinming Wang[4], Suxia Yang[1,2], Shenyang Zhang[1,2], Wanyun Xu[7], Nan Ma[1,2], Zhanyi Zhang[1,2], Bin Jiang[1,2], Hang Su[8], Yafang Cheng[8], Xuemei Wang[1,2], Min Shao[1,2,*], Bin Yuan [1,2,*]

[1] Institute for Environmental and Climate Research, Jinan University, 511443 Guangzhou, China

[2] Guangdong-Hongkong-Macau Joint Laboratory of Collaborative Innovation for Environmental Quality, 511443 Guangzhou, China

[3] School of Environmental Science and Engineering, Qilu University of Technology (Shandong Academy of Sciences), 250353 Jinan, China

[4] State Key Laboratory of Organic Geochemistry and Guangdong Key Laboratory of Environmental Protection and Resources Utilization, Guangzhou Institute of Geochemistry, Chinese Academy of Sciences, 510640 Guangzhou, China

[5] State Joint Key Laboratory of Environmental Simulation and Pollution Control, College of Environmental Sciences and Engineering, Peking University, 100871 Beijing, China

[6] State Key Laboratory of Atmospheric Boundary Physics and Atmospheric Chemistry, Institute of Atmospheric Physics, Chinese Academy of Sciences, 100029 Beijing, China

[7] State Key Laboratory of Severe Weather & Key Laboratory for Atmospheric Chemistry of China Meteorology Administration, Chinese Academy of Meteorological Sciences, 100081 Beijing, China

[8]Multiphase Chemistry Department, Max Planck Institute for Chemistry, Mainz 55128, Germany

*Email: Bin Yuan (byuan@jnu.edu.cn) and Min Shao (mshao@pku.edu.cn)

Abstract: Higher alkanes are a major class of intermediate-volatility organic compounds (IVOCs), which have been proposed to be important precursors of secondary organic aerosols (SOA) in the atmosphere. Accurate estimation of SOA from higher alkanes and their oxidation processes in the atmosphere are limited, partially due to difficulty in their measurements. High-time resolution (10 s) measurements of higher alkanes were performed using NO^+ chemical ionization in proton transfer reaction time-of-flight mass spectrometer (NO^+ PTR-ToF-MS) method at an urban site of Guangzhou in Pearl River Delta (PRD) and at a rural site in North China Plain (NCP), respectively. High concentrations were observed in both environments, with significant diurnal variations. At both sites, SOA production from higher alkanes is estimated from their photochemical losses and SOA yields. Higher alkanes account for significant fractions of SOA formation at the two sites, with average contributions of 7.0±8.0% in Guangzhou and 9.4±9.1% in NCP, which are comparable or even higher than both single-ring aromatics and naphthalenes. The significant contributions of higher alkanes in SOA formation suggests that they should be explicitly included in current models for SOA formation. Our work also highlights the importance of NO^+ PTR-ToF-MS in measuring higher alkanes and quantifying their contributions to SOA formation.

1. Introduction

As important components of fine particles, secondary organic aerosols (SOA) not only affect air quality and climate change, but also threaten human health (An et al., 2019;Zhu et al., 2017;Chowdhury et al., 2018). Recent studies indicate large discrepancies between simulations and observations for SOA (de Gouw et al., 2008;Dzepina et al., 2009;Jiang et al., 2012), which are attributed to limited understanding of complicated chemical and physical processes underlying SOA formation (Hallquist et al., 2009). A volatility basis set (VBS) model was developed to advance SOA modeling by improving the modeling of further multigenerational oxidation processes and incorporating numerous, yet unidentified, low-volatility precursors of SOA (Donahue et al., 2006), which substantially improved the agreement between SOA simulations and observations (Hodzic et al., 2010). However, there are still large uncertainties in current VBS models, including rate constants of oxidation reactions, the change of O/C ratio in oxidation, and the relative importance of functionalization and fragmentation (Ma et al., 2017;Hayes et al., 2015). Explicit consideration of individual or a group of important semi-volatile or intermediate volatile organic compounds (S/I-VOCs) in the SOA model are urgently needed.

Higher alkanes as a major class of IVOCs (roughly corresponding to alkanes with 12-20 carbons) have been proposed as important SOA contributors in urban areas (Robinson et al., 2007;Yuan et al., 2013;Zhao et al., 2014a). In the typical urban areas, higher alkanes are reported to be mainly from vehicle emissions including diesel exhaust (Zhao et al., 2015) and gasoline exhaust (Zhao et al., 2016), corresponding generally to ~4% of NMHCs emissions from on-road vehicles. Higher alkanes are estimated to produce as much as or even more SOA than single-ring aromatics and polycyclic aromatic hydrocarbons from the oxidation of vehicle emissions, based on the chemical compositions measurements of vehicle

exhausts (Zhao et al., 2016, 2015). Based on vehicle exhaust tests, higher alkanes were found to contribute ~37% to diesel exhaust-derived SOA and ~0.8% to gasoline exhaust-derived SOA, respectively (Gentner et al., 2012). Previous model studies suggested that SOA simulation can be significantly improved when higher alkanes were considered in the model (Pye and Pouliot, 2012;Jathar et al., 2014;Wu et al., 2019). Although the concentrations of higher alkanes might be lower than other VOCs classes (e.g. aromatics) in the atmosphere, higher alkanes are found to have much higher SOA yields and the yields increase steadily with carbon number (Lim and Ziemann, 2005;Lim and Ziemann, 2009;Presto et al., 2010b). For a given carbon number, SOA yields of higher alkanes reduce with branching of the carbon chain, especially under high-NO_x conditions (Lim and Ziemann, 2009;Tkacik et al., 2012;Loza et al., 2014).

Higher alkanes have been mainly measured by gas chromatography-based techniques, focusing on the compositions (Gong et al., 2011;Caumo et al., 2018), atmospheric concentration levels (Bi et al., 2003;Anh et al., 2018) and gas-particle partitioning (Xie et al., 2014;Sangiorgi et al., 2014). While most of previous studies collected offline samples (usually 0.5 day-1 week) for GC-based analysis in the laboratory, hourly online measurements of *n*-alkanes using GC-based thermal desorption aerosol gas chromatograph for semi-volatile organic compounds (SV-TAG) was recently developed and applied in ambient air (Zhao et al., 2013). Proton-transfer-reaction mass spectrometry (PTR-MS) using H_3O^+ as reagent ions are capable of measurements for many organic compounds with high time response and sensitivity (de Gouw and Warneke, 2007;Jordan et al., 2009;Yuan et al., 2017b). Although H_3O^+ PTR-MS is responsive to large alkanes (>C8), these alkanes usually fragment into small masses with mass spectra difficult to interpret (Jobson et al., 2005;Gueneron et al., 2015). Recently, PTR-MS using NO^+ as reagent ions was demonstrated to provide fast online measurement of higher alkanes (Koss et al.,

2016;Inomata et al., 2013). The high-time resolution measurements of higher alkanes provide valuable information for SOA estimation, as the dependence of SOA yields on organic aerosol concentrations and other environmental parameters (e.g. temperature) (Lim and Ziemann, 2009;Presto et al., 2010b;Loza et al., 2014;Lamkaddam et al., 2017a) can be taken into account in more detail.

In this study, we utilize NO^+ chemical ionization in PTR-ToF-MS (here referred as NO^+ PTR-ToF-MS) to measure higher alkanes at two different sites in China, one urban site in Pearl River Delta region and one rural site in North China Plain region. We use the datasets along with measurements of other pollutants to estimate contributions to SOA formation from higher alkanes and other SOA precursors. The observation-constrained SOA formation of this study is a step forward upon previous modelling studies, which proposed the important roles of S/I-VOCs (Jiang et al., 2012;Yang et al., 2018;Wu et al., 2019) including higher alkanes (Yuan et al., 2013) in SOA formation in China.

2. Methods

Field campaigns were conducted at an urban site of Guangzhou in the Pearl River Delta (PRD) region during September-November 2018 and at a rural site of Baoding in North China Plain (NCP) during November-December 2018, respectively. The detailed description of the measurement sites can be found in Supporting Information (SI, Figure S1).

2.1 NO^+ PTR-ToF-MS measurements

Proton-transfer-reaction mass spectrometry (PTR-MS) is a technique that allows for fast and sensitive measurements of volatile organic compounds (VOCs) at trace levels in air. PTR-MS using H_3O^+ chemistry has been demonstrated to measure alkenes, aromatics, and even oxygenated VOCs (Yuan et al., 2017a;Wu et al., 2020). Here, PTR-MS with NO^+

chemistry was used to detect higher alkanes, through hydride abstraction by NO^+ forming mass (m-1) ions (m is the molecular mass) (Koss et al., 2016;Inomata et al., 2013).

A commercially available PTR-ToF-MS instrument (Ionicon Analytik, Austria) with a mass resolving power of 4000 m/Δm was used for this work. To generate NO^+ as reagent ions, ultra-high-purity air (5.0 sccm) was directed into the hollow cathode discharge ion source. The pressure of the drift tube was maintained at 3.8 mbar. Voltages of ion source and drift chamber were explored (Figure S2) in the laboratory to optimize the generation of NO^+ ions relative to H_3O^+, O_2^+, and NO_2^+ and minimize alkane fragmentation. The intensities of primary ion NO^+ and impurites (O_2^+, H_3O^+ and NO_2^+) and the ratio of O_2^+ to NO^+ during two campaigns are shown in Figure S3 and Figure S4, respectively. The ratio of O_2^+/NO^+ (Figure S4 **(a)**) is basically stable at 2-4% during the PRD campaign except during Oct. 26-Nov. 2, 2018 (7-10%). For the NCP campaign, the ratio of O_2^+/NO^+ (Figure S4 **(b)**) fluctuates between 10-40% in the early stage of campaign and keeps stable at ~20% in the later stage of the campaign. Such fluctuations are atrributed to the humidity effect in the ambient air (Figure S5). Ion source voltages of Us and Uso were selected as 40 V and 100 V, while Udrift and Udx were set to 470 V and 23.5 V, resulting in an E/N (electric potential intensity relative to gas number density of 60 Td. NO^+ PTR-ToF-MS data was analysed using Tofware software (Tofwerk AG) for high-resolution peak-fitting. A description of the algorithm can be found in Stark et al. (2015) and Timonen et al. (2016). Figure 1 shows the high-resolution peak fitting to the averaged mass spectra on a typical day (12 October 2018) for m/z 169, m/z 211 and m/z 281, at which masses produced by dodecane ($C_{12}H_{25}^+$), pentadecane ($C_{15}H_{31}^+$) and eicosane ($C_{20}H_{41}^+$) are detected. It is observed that the ions from higher alkanes lie at the right-most position at each nominal mass, with signals either the largest or among the largest ions at these nominal masses, which help to achieve high precision for determined signals of higher alkanes from high-resolution peak fitting (Cubison and Jimenez, 2015;Corbin et al., 2015).

In this study, we normalize the raw ion count rate of higher alkanes to the primary ion (NO^+) at a level of 10^6 cps to account for fluctuations of ion source and detector. Calibrations were conducted every 1-2 days under both dry conditions (RH<1%) and ambient humidity conditions using a gas standard with a series of *n*-alkanes (Apel Riemer Environmental Inc.) during NCP campaign (Figure 2(a)). Sensitivities of *n*-alkanes (C8-C15) standards were obtained during the campaign (Figure S6), which is defined as the normalized signal of hydride abstraction ions for each higher alkane at 1 ppbv with a unit of ncps/ppb. The fluctuations of sensitivities during the NCP campaign may be influenced by the variations of O_2^+ signals (Figure 2), because the reactions of O_2^+ with alkanes can be proceeded by both charge transfer and hydride abstraction (Amador et al., 2016) that may affect the ion signals of alkanes with NO^+ reactions. Therefore, we use the daily ambient calibrations results to quantify the concentration of higher alkanes during the NCP campaign to reflect the variations of sensitivity from day to day. For the measurements without daily calibrations, we used closest calibration results according to corresponding ambient O_2^+/NO^+ ratios and ambient humidity. Since we got the alkanes standard at the very late period of the PRD campaign, we did not have the daily calibrations for this campaign. Therefore, we use the sensitivity of each alkane under corresponding O_2^+/NO^+ condition obtained from lab experiments after this campaign and also consider the humidity effects (Figure 3(b, c)) to quantify the concentration of higher alkanes during the PRD campaign. Humidity-dependent behaviours of *n*-alkanes (C8-C15) were performed in the laboratory under different humidity (0-33 mmol/mol) by diluting higher alkanes standard into humidified air to reach approximately 1 ppb mixing ratio. As shown in Figure 3(b, c) and Figure S7 (a), the normalized signal of all product ions (m-1) and the fragment ions of *n*-alkanes (C8-C15) standards are decreasing with the increase of humidity. These decreasing patterns are probably due to the decreasing primary reagent ions (NO^+ and

163 O_2^+) as the humidity increases Figure S7(b). Thus, the humidity correction should be applied
164 for the quantitation of higher alkanes using NO^+ PTR-ToF-MS.

165 The fragmentation patterns for selected *n*-alkanes and their branched isomers are
166 measured with NO^+ PTR-ToF-MS by introducing commercially acquired pure chemicals
167 (Figure S8). Figure 4(a) shows the fractions of hydride abstraction m-1 ions in the mass
168 spectra of C8-C20 *n*-alkanes in NO^+ PTR-ToF-MS. Generally, larger *n*-alkanes show less
169 degree of fragmentation in the mass spectra with higher fractions contributed by m-1 ions.
170 The fractions of m-1 ions account for more than 60% of total ion signals for >C12 *n*-alkanes.
171 We also observe good correlation between the fractions of m-1 ions in mass spectra and the
172 determined sensitivities for C8-C15 *n*-alkanes. As C16-C21 *n*-alkanes exhibit similar degrees
173 of fragmentation as C15, sensitivities of the alkanes were assumed to be same as that of C15
174 *n*-alkane (Figure 4(b)). Comparison of the degree of fragmentation between *n*-alkanes and
175 their branched isomers (Figure S9) show the substituted groups affect little on the degrees of
176 fragmentations for product ions, at least for branched isomers with up to 4 substituted methyl
177 groups. Previous studies demonstrated that the branched alkanes from emissions of fossil fuel-
178 related sources are primarily with one or two alkyl branches (Chan et al., 2013;Isaacman et
179 al., 2012). Therefore, we conclude that the branched isomers of higher alkanes should have
180 similar response factors to their normal analogues. As a result, the concentration of higher
181 alkanes by NO^+ PTR-ToF-MS should be regarded as the summed concentrations of *n*-alkanes
182 and branched alkanes that have the same chemical formulas.

183 Detection limits are calculated as the concentrations at which signal counts are 3 times
184 of standard deviation of measured background counts (Bertram et al., 2011;Yuan et al., 2017b).
185 As shown in Table 1, detection limits are determined to be on the order of 0.7-1.3 ppt for
186 higher alkanes for 1 min integration times. Response time is calculated as the time required
187 to observe a $1/e^2$-signal decay after quick removal of the analyte from the sampled air

(Mikoviny et al., 2010). Response times for various alkanes are better than 1 min, except for C21 alkanes (116 s) (Table1).

During these two campaigns, PTR-ToF-MS automatically switches between H_3O^+ and NO^+ chemistry every 10-20 minutes with a 10 s resolution of measurement. Switching between H_3O^+ and NO^+ ion mode are provided by the PTR-MS Manager (v3.5) software developed by the Ionicon Anlytik (Table S1). The pressures of drift chamber are held constant at 3.8 mbar in both modes during the campaigns (Figure S10(a)). It usually takes <10 s for H_3O^+ ions and ~60 s for NO^+ ions to re-stabilize after automatically switching between the two measurement modes (Figure S10(b)). The ambient measurement data during the transition period (~1 min) was discarded. Ambient air was continuously introduced into PTR-ToF-MS through a Teflon tubing (1/4") with an external pump at 5.0 L/min, with tubing length of ~8 m and ~3 m during the PRD and the NCP campaign, respectively. The inlet tubing was heated all the way to the sampling inlet to avoid water vapour condensation by an insulating tube with a self-controlled heater wire (40 ℃) wrapping outside. The calculated residence time for the inlet was ~3 s for PRD campaign and ~1 s for NCP campaign, respectively. The tubing loss experiments were conducted in the laboratory by introducing standards of higher alkanes (*n*-C8-C15), monoaromatics (benzene, toluene, o-xylene, 1,2,4-trimethylbenzene), isoprenoids (isoprene, α-pinene) and naphthalene into PTR-ToF-MS through a 8 m Teflon tubing (1/4") at room temperature with an external pump at 5.0 L/min (Figure S11). The tubing loss of these compounds is found to be <5% except *n*-C15 (~8%) and naphthalene (~10%). Background measurement of 3 minutes was conducted in each cycle of NO^+ and H_3O^+ measurements by introducing the ambient air into a catalytic converter with a temperature of 367 ℃.

2.2 Other measurements

During the Guangzhou campaign, an online GC-MS/FID system was used to measure C2-C11 *n*-alkanes, alkenes and aromatics with a time resolution of one hour (Yuan et al., 2012). Non-refractory components in particulate matter with diameter less than 1μm (PM_1) including nitrate, sulfate, ammonium, chloride, and organics were measured with an Aerodyne high-resolution time-of-flight aerosol mass spectrometric (HR-ToF-AMS) and a time-of-flight aerosol chemical speciation monitor (ToF-ACSM) in PRD and NCP, respectively. Trace gaseous species (CO, NO, NO_2, O_3, and SO_2) were measured using commercial gas analyzers (Thermo Scientific). Photolysis frequencies were measured using a spectroradiometer (PFS-100, Focused Photonics Inc.). In addition, temperature, pressure, relative humidity and wind were continuously measured during two campaigns.

3. Results and Discussion

3.1 Ambient concentrations and diurnal variations of higher alkanes

Although NO^+ chemistry has been shown to be valuable in measuring many organic species, the applications in real atmosphere of different environments are still rare (Koss et al., 2016). Here, we compared the measurements of various VOCs from NO^+ PTR-ToF-MS with both H_3O^+ PTR-ToF-MS and GC-MS/FID during the two campaigns. Overall, good agreements between PTR-ToF-MS (both H_3O^+ and NO^+ chemistry) and GC-MS/FID are obtained for aromatics and oxygenated VOCs except benzene (Figure S12, S13). Benzene measurements in H_3O^+ chemistry show large difference with benzene measured from NO^+ chemistry in the earlier period of PRD campaign (11 Sep.-14 Oct. 2018), but good agreement was obtained for the rest of measurement period. Considering good agreement of benzene between NO^+ PTR-ToF-MS and GC-MS/FID, we used benzene data from NO^+ measurement in this study. The time series and diurnal variations of alkanes (C8-C11) between NO^+ PTR-ToF-MS and GC-MS/FID are shown in Figure 5 (and Figure S14). Similar temporal trends for these alkanes are

observed from the two instruments. However, the concentrations at each carbon number from NO^+ PTR-ToF-MS are ~3-6 times those from GC-MS/FID. This is expected, as dozens to hundreds of isomers exists for alkanes with carbon number at this range (Goldstein and Galbally, 2007) and GC-MS/FID only measured one or a few isomers. Based on measurements from NO^+ PTR-ToF-MS and GC-MS/FID, we compute the molar concentration fractions of *n*-alkanes for each carbon number (Figure 6 and Table S1). We found the fractions are in the range of 11%-21% for carbon number of 8-11, which are comparable with results of ambient air in California and vehicle exhausts (Figure 6 and Table S2) (Chan et al., 2013;Gentner et al., 2012). These results indicate the importance of branched alkanes in concentrations of higher alkanes and their potential contributions to SOA formation. It also has strong implication for the merits of NO^+ PTR-ToF-MS in measuring sum of the alkanes with the same formula for estimation of SOA contributions, as discussed later.

Table 2 summarizes means and standard deviations of concentrations of C8-C21 higher alkanes measured in PRD and in NCP, respectively. The mean concentrations of *n*-alkanes measured at a suburban site in Paris (Ait-Helal et al., 2014) and an urban site in Pasadena, U.S. are also included in Table 1 for comparison. According to the fraction of *n*-alkanes, the mean concentrations of *n*-alkanes in China are found to be comparable to that from Paris and higher than in Pasadena. In general, concentrations of higher alkanes concentration decrease with the increase of carbon number, with octanes (C8) at ~0.5 ppb and heneicosanes (C21) at ~0.002 ppb. This decreasing pattern of carbon distribution are as the results of lower emissions from sources (Gentner et al., 2012), larger reactivity towards OH radicals (Atkinson et al., 2008;Keyte et al., 2013) and larger fractions partitioning to particles (Liang et al., 1997;Xie et al., 2014;Zhao et al., 2013) in the atmosphere.

The diurnal variations of selected higher alkanes are shown in Figure 7. C12 alkanes and C15 alkanes exhibit similarly strong diurnal variations at both sites, with a relatively

high levels at night and minimum concentrations detected in the late afternoon at both sites. Such diurnal patterns are consistent with other primary VOCs species (e.g. aromatics). In PRD, the diurnal variations of higher alkanes were as the result of faster chemical removal in the daytime and shallow boundary layer heights at night. Since OH concentrations in NCP during winter were much lower than that in PRD during autumn (Figure S15), diurnal variations of higher alkanes in NCP were mainly influenced by the change of boundary layer.The diurnal profiles of other higher alkanes are similar to C12 and C15 alkanes.

3.2 Estimation of the contributions of higher alkanes to SOA formation

A time-resolved approach based on consideration of photo-oxidation processes with OH radical (Ait-Helal et al., 2014) was applied to estimate contributions of higher alkanes to SOA during these two campaigns. In order to evaluate the relative importance to SOA from different precursors, the same method was also used for monoaromatics, naphthalenes, and isoprenoids.

This method considers the amount of chemical removal based on the parameterized photochemical age, which was widely used to quantify contributions of different VOC precursors to SOA formation (Zhao et al., 2014a;Ait-Helal et al., 2014;de Gouw et al., 2009). The contributions to SOA formation from different compounds are determined by the ratios of calculated SOA production amounts from individual precursors (SI, Appendix 2) and SOA concentrations derived from factor analysis of OA measurements by AMS (SI, Appendix 3). In this method, SOA formation for a given compound can be estimated by

$$[SOA_i]_t = [VOC_i]_t \times (e^{kVOC_i \times ([OH] \times \Delta t)} - 1) \times Yield_i \quad (1)$$

where $[SOA_i]_t$ is the calculated SOA production (μg m^{-3}) for a given specific compound VOC_i at time t, $[VOC_i]_t$ is the VOC_i concentration measured at time t (μg m^{-3}), $Yield_i$ is the SOA

yield data summarized from chamber studies, k_{VOC_i} is the rate constant of VOC_i with the OH radical (cm^3 $molecule^{-1}$ s^{-1}). The OH exposure, $[OH] \times \Delta t$ (molecules cm^{-3} s), is estimated by the ratio m+p-xylene and ethylbenzene with different reactivity for anthropogenic VOCs and by the oxidation processes of isoprene for biogenic VOCs, respectively (Apel et al., 2002;Roberts et al., 2006) (see details in SI, Appendix 4 and Figure S16). Since biogenic emissions were pretty weak during cold winter (mean temperature 0.5±3.6 °C) during NCP campaign, measured concentrations of isoprene and monoterpenes are attributed to be of anthropogenic origin during the winter campaign in NCP campaign, especially given the fact that they showed similar variations, diurnal profiles and strong correlation with CO and anthropogenic VOCs species (Figure S17). A previous study in Helsinki also found the importance of anthropogenic emission in monoterpene concentrations (Hellén et al., 2012).

Based on equation (1), SOA production from higher alkanes (C8-C21 alkanes), monoaromatics (benzene, toluene, C8 aromatics, C9 aromatics, styrene), naphthalenes (naphthalene, methylnaphthalenes, dimethylnaphthalenes) and isoprenoids (isoprene, monoterpenes) were calculated. The concentration data of higher alkanes, isoprenoids and benzene were taken from measurements of NO^+ PTR-ToF-MS. The concentration data of naphthalenes (Figure S18) and monoaromatics except benzene were taken from measurements of H_3O^+ PTR-ToF-MS. The detail about the H_3O^+ PTR-ToF-MS measurements can be found in Wu et al. (2020). The OH reaction rate constant of each compound was taken from literature (Atkinson, 2003). SOA yield data used here for higher alkanes (Lim and Ziemann, 2009;Presto et al., 2010a;Loza et al., 2014;Lamkaddam et al., 2017b), monoaromatics (Li et al., 2016;Ng et al., 2007;Tajuelo et al., 2019), naphthalenes (Chan et al., 2009) and isoprenoids (Ahlberg et al., 2017;Carlton et al., 2009;Edney et al., 2005;Kleindienst et al., 2006;Pandis et al., 1991) were summarized from reported values in the literature, with the consideration of the influence of organic aerosol concentration (Figure S19) to SOA yields

(Donahue et al., 2006) (Figure S20-21). SOA yields under high NO_x conditions are used in this study, as relatively high NO_x concentrations in PRD (42.6±33.7 ppb) and in NCP (81.7±57.0 ppb) (Figure S22) would cause RO_2 radicals from organic compounds mainly reacting with NO (Bahreini et al., 2009).

Both OH reaction rate constants and SOA yields of *n*-alkanes reported in the literature are applied for higher alkanes, as most of the chamber studies have focused on n-alkanes. The OH reaction rate constants of branched alkanes are higher than those of n-alkanes, while their SOA yields are lower than *n*-alkanes, of which both depending on chemical structures of the carbon backbone (Lim and Ziemann, 2009;Tkacik et al., 2012;Loza et al., 2014). The combined effects are hard to evaluate due to limited data, but the two effects can partially (if not all) cancel out. As shown above, temperature (mean temperature 0.5±3.6 °C) in NCP winter campaign was significantly lower than the temperature (usually 25 °C) at which SOA yields are derived from chamber studies. Temperature can significantly influence SOA yields, with higher yields at lower temperature (Takekawa et al., 2003;Lamkaddam et al., 2017b). It might cause underestimation of SOA production from various precursors in winter of NCP.

The calculated results of SOA production for different higher alkanes are shown in Figure 8. Although lower concentrations of heavier alkanes were observed for both campaigns, the calculated SOA production are largest for C12-C18 (Figure 8(b)). This is because of two reasons: (1) Alkanes with larger carbon number have larger SOA yields. The calculated average SOA yields (Table S3) during the two campaigns are both larger than 0.2 for >C12 alkanes and increase to near unity for C20-C21 alkanes. (2) Larger alkanes are relatively more reactive than lighter ones, which results in larger proportions of calculated concentrations that have been chemically consumed in the atmosphere. The distribution of contributions from alkanes with different carbon number to SOA formation shown here is in good agreement with the previous results referred from volatility calculation for precursors

(de Gouw et al., 2011;Liggio et al., 2016). The magnitudes of photochemical processes are apparently different between the two campaigns, with larger calculated OH exposure in the PRD campaign in autumn than the NCP campaign in winter (Figure S16). Consequently, the calculated chemical losses of alkane concentrations and their SOA production are much higher in PRD, though measured alkane concentrations are comparable during the two campaigns.

Along with higher alkanes, SOA production for monoaromatics, naphthalenes and isoprenoids are shown in Figure 9 (and Figure S23-25). Compared to monoaromatics, higher alkanes are associated with lower concentrations (Figure S26). However, higher alkanes play an important role in SOA formation due to their high SOA yields (Figure S27). The total average SOA production from C8-C21 alkanes are 0.6±0.8 μg m^{-3} and 0.7±0.8 μg m^{-3} in PRD and NCP, respectively. The formed SOA from higher alkanes account for 7.0±8.0% and 9.4±9.1% of SOA formation in PRD and NCP, respectively. The contributions of monoaromatics to SOA formation are 6.2±7.7% and 9.4±17.4% in PRD and NCP, respectively. Naphthalenes have been proposed to be important precursors of SOA from laboratory chamber studies (Kleindienst et al., 2012). In this study, we determine 2.8±4.6% of SOA in PRD and 11.1±14.3% of SOA in NCP are contributed by naphthalenes. The SOA contribution from naphthalenes determined for NCP is comparable to the results (10.2±1.0%) obtained during haze events in Beijing in a recent study (Huang et al., 2019). Significant contribution from monoterpenes to SOA (8.7±14.6%) is observed in NCP. As mentioned above, we attribute these isoprene and monoterpenes to anthropogenic emissions in this region. The SOA precursors considered in this study in total could explain 14.9%-29.0% and 16.4-125.3% of SOA formation in PRD and NCP, respectively. The influence of chamber-based vapour wall losses on SOA yields was examined in previous studies (Zhang et al., 2014) and the results show that the literature reported SOA yields are low by factors of ~1.1-2.2 for the

high NO_x conditions (Table S4). This suggests that the SOA estimations in this study might be correspondingly underestimated. The lower explained percentages of SOA formation during the highly polluted periods and during the daytime in NCP (Figure S23(b)) imply that some other SOA precursors or formation pathways (e.g. aqueous reactions) are contributing significantly to SOA formation of the strong haze pollution in NCP. Compared to a previous study in northern China (Yuan et al., 2013), the missing gap of SOA formation declined after explicitly considering higher alkanes and naphthalenes in SOA production.

As shown in Figure 9, we find that C8-C21 higher alkanes contribute significantly to SOA formation at both an urban site in autumn of PRD and a rural site in winter of NCP. The contributions from higher alkanes are either comparable or higher than both monoaromatics and naphthalenes. Another estimation method by considering SOA instantaneous production rates obtained similar results (Figure S28), which confirms the results from the photochemical age based on parameterization method shown above. The importance of higher alkanes in SOA formation has been also proposed in several previous SOA modelling studies (Pye and Pouliot, 2012;Zhao et al., 2014b). These results, along with our results from observations in ambient atmosphere, underline that the inclusion of higher alkanes in SOA models in the atmosphere should be considered if possible.

4. Concluding remarks

In this study, we utilized a NO^+ PTR-ToF-MS to measure C8-C21 alkanes in two different environments in China. Based on a series of laboratory experiments, we show that NO^+ PTR-ToF-MS can provide online measurements of higher alkanes with high accuracy and fast response. The measured concentrations of higher alkanes were relatively high during the two campaigns. The diurnal profiles of higher alkanes are similar to anthropogenic VOCs, implying they are emitted from anthropogenic sources.

On the basis of measurements of higher alkanes by NO^+ PTR-ToF-MS, we successfully take into account their contributions in SOA formation. The time-resolved measurements of higher alkanes by NO^+ PTR-ToF-MS provide the opportunity to accurately apply the photochemical age-based parameterization method. As there is no separation before detection in PTR-ToF-MS, the measured concentrations of NO^+ PTR-ToF-MS represent all of the compounds that contribute to the product ions (m-1 ions), which include concentrations from both *n*-alkanes and branched alkanes. With the total concentration of both *n*-alkanes and branched alkanes quantified, the contribution from higher alkanes at each carbon number can be estimated as a whole. This is an important supplementary method to the traditional analytical method by GC techniques for higher alkanes, as fully chemical separation and detection of numerous isomers of higher alkanes remain as a challenge, even using the most advanced GC×GC-ToF-MS instruments (Chan et al., 2013;Alam et al., 2016).

Higher alkanes were found to have significant contributions to SOA in both PRD and NCP regions with a similar or even higher contributions than that of monoaromatics and naphthalenes. The importance of higher alkanes to SOA formation also call for more work to investigate emissions and chemistry of these compounds in the atmosphere. It was shown that fossil-related combustions such as vehicle exhausts are major sources for higher alkanes (Zhao et al., 2016). While, recent studies have shown that non-combustion sources, such as the use of solvents, have a potentially significant impact on high-alkane emissions (McDonald et al., 2018;Khare and Gentner, 2018). However, such quantitative information on emissions of higher alkanes is still limited. The measurements of higher alkanes by NO^+ PTR-ToF-MS with fast response could help to fill these research gaps.

Acknowledgements

This work was supported by the National Key R&D Plan of China (grant No. 2018YFC0213904, 2016YFC0202206), the National Natural Science Foundation of China (grant No. 41877302), Guangdong Natural Science Funds for Distinguished Young Scholar (grant No. 2018B030306037), Guangdong Provincial Key R&D Plan (grant No. 2019B110206001), Guangdong Soft Science Research Program (grant No. 2019B101001005) and Guangdong Innovative and Entrepreneurial Research Team Program (grant No. 2016ZT06N263). Weiwei Hu and Wei Chen were supported by National Natural Science Foundation of China (grant No. 41875156). The authors gratefully acknowledge the science team for their technical support and discussions during the campaigns in PRD and NCP.

Data availability

Data is available from the authors upon request

Competing interests

The authors declare that they have no conflicts of interest

Author contributions

BY and MS designed the research. CMW, CHW, SHW, JPQ, BLW, WC, CW, WS and WYX contributed to data collection. CMW performed the data analysis, with contributions from ZLW, WWH, SXY and CSY. CMW and BY prepared the manuscript with contributions from other authors. All the authors reviewed the manuscript.

References

Ahlberg, E., Falk, J., Eriksson, A., Holst, T., Brune, W. H., Kristensson, A., Roldin, P., and Svenningsson, B.: Secondary organic aerosol from VOC mixtures in an oxidation flow reactor, Atmospheric Environment, 161, 210-220, 10.1016/j.atmosenv.2017.05.005, 2017.

Ait-Helal, W., Borbon, A., Sauvage, S., de Gouw, J. A., Colomb, A., Gros, V., Freutel, F., Crippa, M., Afif, C., Baltensperger, U., Beekmann, M., Doussin, J. F., Durand-Jolibois, R., Fronval, I., Grand, N., Leonardis, T., Lopez, M., Michoud, V., Miet, K., Perrier, S., Prevot, A. S. H., Schneider, J., Siour, G., Zapf, P., and Locoge, N.: Volatile and intermediate volatility organic compounds in suburban Paris: variability, origin and importance for SOA formation, Atmospheric Chemistry and Physics, 14, 10439-10464, 10.5194/acp-14-10439-2014, 2014.

Alam, M. S., Stark, C., and Harrison, R. M.: Using Variable Ionization Energy Time-of-Flight Mass Spectrometry with Comprehensive GCxGC To Identify Isomeric Species, Analytical Chemistry, 88, 4211-4220, 10.1021/acs.analchem.5b03122, 2016.

Amador, O., Misztal, P., Weber, R., Worton, D., Zhang, H., Drozd, G., and Goldstein, A.: Sensitive detection of n -alkanes using a mixed ionization mode proton-transfer-reaction mass spectrometer, Atmospheric Measurement Techniques, 9, 5315-5329, 10.5194/amt-9-5315-2016, 2016.

An, Z., Huang, R. J., Zhang, R., Tie, X., Li, G., Cao, J., Zhou, W., Shi, Z., Han, Y., Gu, Z., and Ji, Y.: Severe haze in northern China: A synergy of anthropogenic emissions and atmospheric processes, Proc Natl Acad Sci U S A, 116, 8657-8666, 10.1073/pnas.1900125116, 2019.

Anh, H. Q., Tomioka, K., Tue, N. M., Tuyen, L. H., Chi, N. K., Minh, T. B., Viet, P. H., and Takahashi, S.: A preliminary investigation of 942 organic micro-pollutants in the atmosphere in waste processing and urban areas, northern Vietnam: Levels, potential sources, and risk assessment, Ecotoxicol. Environ. Saf., 167, 354-364, 2018.

Apel, E. C., Riemer, D. D., Hills, A., Baugh, W., Orlando, J., Faloona, I., Tan, D., Brune, W., Lamb, B., Westberg, H., Carroll, M. A., Thornberry, T., and Geron, C. D.: Measurement and interpretation of isoprene fluxes and isoprene, methacrolein, and methyl vinyl ketone mixing ratios at the PROPHET

452 site during the 1998 Intensive, Journal of Geophysical Research: Atmospheres, 107, ACH 7-1-ACH 7-
453 15, 10.1029/2000JD000225, 2002.
454 Atkinson, R.: Kinetics of the gas-phase reactions of OH radicals with alkanes and cycloalkanes,
455 Atmospheric Chemistry and Physics, 3, 2233-2307, 10.5194/acp-3-2233-2003, 2003.
456 Atkinson, R., Arey, J., and Aschmann, S. M.: Atmospheric chemistry of alkanes: Review and recent
457 developments, Atmospheric Environment, 42, 5859-5871, 10.1016/j.atmosenv.2007.08.040, 2008.
458 Bertram, T., Kimmel, J., Crisp, T., Ryder, O., Yatavelli, R., Thornton, J., Cubison, M., Gonin, M., and
459 Worsnop, D.: A field-deployable, chemical ionization time-of-flight mass spectrometer, Atmospheric
460 Measurement Techniques, 4, 1471-1479, 10.5194/amt-4-1471-2011, 2011.
461 Bi, X. H., Sheng, G. Y., Peng, P., Chen, Y. J., Zhang, Z. Q., and Fu, J. M.: Distribution of particulate-
462 and vapor-phase n-alkanes and polycyclic aromatic hydrocarbons in urban atmosphere of Guangzhou,
463 China, Atmospheric Environment, 37, 289-298, 10.1016/s1352-2310(02)00832-4, 2003.
464 Carlton, A. G., Wiedinmyer, C., and Kroll, J. H.: A review of Secondary Organic Aerosol (SOA)
465 formation from isoprene, Atmospheric Chemistry and Physics, 9, 4987-5005, DOI 10.5194/acp-9-4987-
466 2009, 2009.
467 Caumo, S., Vicente, A., Custodio, D., Alves, C., and Vasconcellos, P.: Organic compounds in
468 particulate and gaseous phase collected in the neighbourhood of an industrial complex in Sao Paulo
469 (Brazil), Air Quality Atmosphere and Health, 11, 271-283, 10.1007/s11869-017-0531-7, 2018.
470 Chan, A. W. H., Kautzman, K. E., Chhabra, P. S., Surratt, J. D., Chan, M. N., Crounse, J. D., Kuerten,
471 A., Wennberg, P. O., Flagan, R. C., and Seinfeld, J. H.: Secondary organic aerosol formation from
472 photooxidation of naphthalene and alkylnaphthalenes: implications for oxidation of intermediate
473 volatility organic compounds (IVOCs), Atmospheric Chemistry and Physics, 9, 3049-3060,
474 10.5194/acp-9-3049-2009, 2009.
475 Chan, A. W. H., Isaacman, G., Wilson, K. R., Worton, D. R., Ruehl, C. R., Nah, T., Gentner, D. R.,
476 Dallmann, T. R., Kirchstetter, T. W., Harley, R. A., Gilman, J. B., Kuster, W. C., deGouw, J. A.,
477 Offenberg, J. H., Kleindienst, T. E., Lin, Y. H., Rubitschun, C. L., Surratt, J. D., Hayes, P. L., Jimenez,
478 J. L., and Goldstein, A. H.: Detailed chemical characterization of unresolved complex mixtures in
479 atmospheric organics: Insights into emission sources, atmospheric processing, and secondary organic

480 aerosol formation, Journal of Geophysical Research-Atmospheres, 118, 6783-6796,
481 10.1002/jgrd.50533, 2013.
482 Chowdhury, P. H., He, Q., Male, T. L., Brune, W. H., Rudich, Y., and Pardo, M.: Exposure of Lung
483 Epithelial Cells to Photochemically Aged Secondary Organic Aerosol Shows Increased Toxic Effects,
484 Environmental Science & Technology Letters, 5, 424-430, 10.1021/ars.estlett.8b00256, 2018.
485 Corbin, J. C., Othman, A., D. Allan, J., R. Worsnop, D., D. Haskins, J., Sierau, B., Lohmann, U., and
486 A. Mensah, A.: Peak-fitting and integration imprecision in the Aerodyne aerosol mass spectrometer:
487 effects of mass accuracy on location-constrained fits, Atmos. Meas. Tech., 8, 4615-4636, 10.5194/amt-
488 8-4615-2015, 2015.
489 Cubison, M. J., and Jimenez, J. L.: Statistical precision of the intensities retrieved from constrained
490 fitting of overlapping peaks in high-resolution mass spectra, Atmos. Meas. Tech., 8, 2333-2345,
491 10.5194/amt-8-2333-2015, 2015.
492 de Gouw, J., and Warneke, C.: Measurements of volatile organic compounds in the earths atmosphere
493 using proton-transfer-reaction mass spectrometry, Mass Spectrometry Reviews, 26, 223-257,
494 10.1002/mas.20119, 2007.
495 de Gouw, J. A., Brock, C. A., Atlas, E. L., Bates, T. S., Fehsenfeld, F. C., Goldan, P. D., Holloway, J.
496 S., Kuster, W. C., Lerner, B. M., Matthew, B. M., Middlebrook, A. M., Onasch, T. B., Peltier, R. E.,
497 Quinn, P. K., Senff, C. J., Stohl, A., Sullivan, A. P., Trainer, M., Warneke, C., Weber, R. J., and
498 Williams, E. J.: Sources of particulate matter in the northeastern United States in summer: 1. Direct
499 emissions and secondary formation of organic matter in urban plumes, Journal of Geophysical
500 Research-Atmospheres, 113, 10.1029/2007jd009243, 2008.
501 de Gouw, J. A., Welsh-Bon, D., Warneke, C., Kuster, W. C., Alexander, L., Baker, A. K., Beyersdorf,
502 A. J., Blake, D. R., Canagaratna, M., Celada, A. T., Huey, L. G., Junkermann, W., Onasch, T. B.,
503 Salcido, A., Sjostedt, S. J., Sullivan, A. P., Tanner, D. J., Vargas, O., Weber, R. J., Worsnop, D. R., Yu,
504 X. Y., and Zaveri, R.: Emission and chemistry of organic carbon in the gas and aerosol phase at a sub-
505 urban site near Mexico City in March 2006 during the MILAGRO study, Atmospheric Chemistry and
506 Physics, 9, 3425-3442, 10.5194/acp-9-3425-2009, 2009.

de Gouw, J. A., Middlebrook, A. M., Warneke, C., Ahmadov, R., Atlas, E. L., Bahreini, R., Blake, D. R., Brock, C. A., Brioude, J., Fahey, D. W., Fehsenfeld, F. C., Holloway, J. S., Le Henaff, M., Lueb, R. A., McKeen, S. A., Meagher, J. F., Murphy, D. M., Paris, C., Parrish, D. D., Perring, A. E., Pollack, I. B., Ravishankara, A. R., Robinson, A. L., Ryerson, T. B., Schwarz, J. P., Spackman, J. R., Srinivasan, A., and Watts, L. A.: Organic aerosol formation downwind from the Deepwater Horizon oil spill, Science, 331, 1295-1299, 10.1126/science.1200320, 2011.

Donahue, N. M., Robinson, A. L., Stanier, C. O., and Pandis, S. N.: Coupled partitioning, dilution, and chemical aging of semivolatile organics, Environmental Science & Technology, 40, 2635-2643, 10.1021/es052297c, 2006.

Dzepina, K., Volkamer, R. M., Madronich, S., Tulet, P., Ulbrich, I. M., Zhang, Q., Cappa, C. D., Ziemann, P. J., and Jimenez, J. L.: Evaluation of recently-proposed secondary organic aerosol models for a case study in Mexico City, Atmospheric Chemistry and Physics, 9, 5681-5709, 10.5194/acp-9-5681-2009, 2009.

Edney, E. O., Kleindienst, T. E., Jaoui, M., Lewandowski, M., Offenberg, J. H., Wang, W., and Claeys, M.: Formation of 2-methyl tetrols and 2-methylglyceric acid in secondary organic aerosol from laboratory irradiated isoprene/NOX/SO2/air mixtures and their detection in ambient PM2.5 samples collected in the eastern United States, Atmospheric Environment, 39, 5281-5289, https://doi.org/10.1016/j.atmosenv.2005.05.031, 2005.

Gentner, D. R., Isaacman, G., Worton, D. R., Chan, A. W. H., Dallmann, T. R., Davis, L., Liu, S., Day, D. A., Russell, L. M., Wilson, K. R., Weber, R., Guha, A., Harley, R. A., and Goldstein, A. H.: Elucidating secondary organic aerosol from diesel and gasoline vehicles through detailed characterization of organic carbon emissions, Proceedings of the National Academy of Sciences of the United States of America, 109, 18318-18323, 10.1073/pnas.1212272109, 2012.

Goldstein, A. H., and Galbally, I. E.: Known and Unexplored Organic Constituents in the Earth's Atmosphere, Environmental Science & Technology, 41, 1514-1521, 10.1021/es072476p, 2007.

Gong, P., Wang, X., and Yao, T.: Ambient distribution of particulate- and gas-phase n-alkanes and polycyclic aromatic hydrocarbons in the Tibetan Plateau, Environmental Earth Sciences, 64, 1703-1711, 10.1007/s12665-011-0974-3, 2011.

Gueneron, M., Erickson, M. H., VanderSchelden, G. S., and Jobson, B. T.: PTR-MS fragmentation patterns of gasoline hydrocarbons, International Journal of Mass Spectrometry, 379, 97-109, 10.1016/j.ijms.2015.01.001, 2015.

Hallquist, M., Wenger, J. C., Baltensperger, U., Rudich, Y., Simpson, D., Claeys, M., Dommen, J., Donahue, N. M., George, C., Goldstein, A. H., Hamilton, J. F., Herrmann, H., Hoffmann, T., Iinuma, Y., Jang, M., Jenkin, M. E., Jimenez, J. L., Kiendler-Scharr, A., Maenhaut, W., McFiggans, G., Mentel, T. F., Monod, A., Prevot, A. S. H., Seinfeld, J. H., Surratt, J. D., Szmigielski, R., and Wildt, J.: The formation, properties and impact of secondary organic aerosol: current and emerging issues, Atmospheric Chemistry and Physics, 9, 5155-5236, 10.5194/acp-9-5155-2009, 2009.

Hayes, P. L., Carlton, A. G., Baker, K. R., Ahmadov, R., Washenfelder, R. A., Alvarez, S., Rappenglueck, B., Gilman, J. B., Kuster, W. C., de Gouw, J. A., Zotter, P., Prevot, A. S. H., Szidat, S., Kleindienst, T. E., Offenberg, J. H., Ma, P. K., and Jimenez, J. L.: Modeling the formation and aging of secondary organic aerosols in Los Angeles during CalNex 2010, Atmospheric Chemistry and Physics, 15, 5773-5801, 10.5194/acp-15-5773-2015, 2015.

Hellén, H., Tykkä, T., and Hakola, H.: Importance of monoterpenes and isoprene in urban air in northern Europe, Atmospheric Environment, 59, 59-66, https://doi.org/10.1016/j.atmosenv.2012.04.049, 2012.

Hodzic, A., Jimenez, J. L., Madronich, S., Canagaratna, M. R., DeCarlo, P. F., Kleinman, L., and Fast, J.: Modeling organic aerosols in a megacity: potential contribution of semi-volatile and intermediate volatility primary organic compounds to secondary organic aerosol formation, Atmospheric Chemistry and Physics, 10, 5491-5514, 10.5194/acp-10-5491-2010, 2010.

Huang, G., Liu, Y., Shao, M., Li, Y., Chen, Q., Zheng, Y., Wu, Z., Liu, Y., Wu, Y., Hu, M., Li, X., Lu, S., Wang, C., Liu, J., Zheng, M., and Zhu, T.: Potentially Important Contribution of Gas-Phase Oxidation of Naphthalene and Methylnaphthalene to Secondary Organic Aerosol during Haze Events in Beijing, Environmental Science & Technology, 53, 1235-1244, 10.1021/acs.est.8b04523, 2019.

Inomata, S., Tanimoto, H., and Yamada, H.: Mass Spectrometric Detection of Alkanes Using NO+ Chemical Ionization in Proton-transfer-reaction Plus Switchable Reagent Ion Mass Spectrometry, Chemistry Letters, 43, 538-540, 10.1246/cl.131105, 2013.

562 Isaacman, G., Wilson, K. R., Chan, A. W. H., Worton, D. R., Kimmel, J. R., Nah, T., Hohaus, T., Gonin,
563 M., Kroll, J. H., Worsnop, D. R., and Goldstein, A. H.: Improved Resolution of Hydrocarbon Structures
564 and Constitutional Isomers in Complex Mixtures Using Gas Chromatography-Vacuum Ultraviolet-
565 Mass Spectrometry, Analytical Chemistry, 84, 2335-2342, 10.1021/ac2030464, 2012.
566 Jathar, S. H., Gordon, T. D., Hennigan, C. J., Pye, H. O. T., Pouliot, G., Adams, P. J., Donahue, N. M.,
567 and Robinson, A. L.: Unspeciated organic emissions from combustion sources and their influence on
568 the secondary organic aerosol budget in the United States, Proceedings of the National Academy of
569 Sciences of the United States of America, 111, 10473-10478, 10.1073/pnas.1323740111, 2014.
570 Jiang, F., Liu, Q., Huang, X., Wang, T., Zhuang, B., and Xie, M.: Regional modeling of secondary
571 organic aerosol over China using WRF/Chem, Journal of Aerosol Science, 43, 57-73,
572 10.1016/j.jaerosci.2011.09.003, 2012.
573 Jobson, B. T., Alexander, M. L., Maupin, G. D., and Muntean, G. G.: On-line analysis of organic
574 compounds in diesel exhaust using a proton transfer reaction mass spectrometer (PTR-MS),
575 International Journal of Mass Spectrometry, 245, 78-89, 10.1016/j.ijms.2005.05.009, 2005.
576 Jordan, A., Haidacher, S., Hanel, G., Hartungen, E., Herbig, J., Maerk, L., Schottkowsky, R., Seehauser,
577 H., Sulzer, P., and Maerk, T. D.: An online ultra-high sensitivity Proton-transfer-reaction mass-
578 spectrometer combined with switchable reagent ion capability (PTR+SRI-MS), International Journal of
579 Mass Spectrometry, 286, 32-38, 10.1016/j.ijms.2009.06.006, 2009.
580 Keyte, I. J., Harrison, R. M., and Lammel, G.: Chemical reactivity and long-range transport potential
581 of polycyclic aromatic hydrocarbons - a review, Chemical Society Reviews, 42, 9333-9391,
582 10.1039/c3cs60147a, 2013.
583 Khare, P., and Gentner, D. R.: Considering the future of anthropogenic gas-phase organic compound
584 emissions and the increasing influence of non-combustion sources on urban air quality, Atmospheric
585 Chemistry and Physics, 18, 5391-5413, 10.5194/acp-18-5391-2018, 2018.
586 Kleindienst, T. E., Edney, E. O., Lewandowski, M., Offenberg, J. H., and Jaoui, M.: Secondary Organic
587 Carbon and Aerosol Yields from the Irradiations of Isoprene and α-Pinene in the Presence of NOx and
588 SO2, Environmental Science & Technology, 40, 3807-3812, 10.1021/es052446r, 2006.

589 Kleindienst, T. E., Jaoui, M., Lewandowski, M., Offenberg, J. H., and Docherty, K. S.: The formation
590 of SOA and chemical tracer compounds from the photooxidation of naphthalene and its methyl analogs
591 in the presence and absence of nitrogen oxides, Atmospheric Chemistry and Physics, 12, 8711-8726,
592 10.5194/acp-12-8711-2012, 2012.
593 Koss, A. R., Warneke, C., Yuan, B., Coggon, M. M., Veres, P. R., and de Gouw, J. A.: Evaluation of
594 NO+ reagent ion chemistry for online measurements of atmospheric volatile organic compounds,
595 Atmospheric Measurement Techniques, 9, 2909-2925, 10.5194/amt-9-2909-2016, 2016.
596 Lamkaddam, H., Gratien, A., Pangui, E., Cazaunau, M., Picquet-Varrault, B., and Doussin, J.-F.: High-
597 NOx Photooxidation of n-Dodecane: Temperature Dependence of SOA Formation, Environmental
598 Science & Technology, 51, 192-201, 10.1021/acs.est.6b03821, 2017a.
599 Lamkaddam, H., Gratien, A., Pangui, E., Cazaunau, M., Picquet-Varrault, B., and Doussin, J. F.: High-
600 NOx Photooxidation of n-Dodecane: Temperature Dependence of SOA Formation, Environ Sci
601 Technol, 51, 192-201, 10.1021/acs.est.6b03821, 2017b.
602 Li, L., Tang, P., Nakao, S., Kacarab, M., and Cocker, D. R., 3rd: Novel Approach for Evaluating
603 Secondary Organic Aerosol from Aromatic Hydrocarbons: Unified Method for Predicting Aerosol
604 Composition and Formation, Environ Sci Technol, 50, 6249-6256, 10.1021/acs.est.5b05778, 2016.
605 Liang, C., Pankow, J. F., Odum, J. R., and Seinfeld, J. H.: Gas/Particle Partitioning of Semivolatile
606 Organic Compounds To Model Inorganic, Organic, and Ambient Smog Aerosols, Environmental
607 Science & Technology, 31, 3086-3092, 10.1021/es9702529, 1997.
608 Liggio, J., Li, S.-M., Hayden, K., Taha, Y. M., Stroud, C., Darlington, A., Drollette, B. D., Gordon, M.,
609 Lee, P., Liu, P., Leithead, A., Moussa, S. G., Wang, D., O'Brien, J., Mittermeier, R. L., Brook, J. R.,
610 Lu, G., Staebler, R. M., Han, Y., Tokarek, T. W., Osthoff, H. D., Makar, P. A., Zhang, J., L. Plata, D.,
611 and Gentner, D. R.: Oil sands operations as a large source of secondary organic aerosols, Nature, 534,
612 91-94, 10.1038/nature17646, 2016.
613 Lim, Y. B., and Ziemann, P. J.: Products and mechanism of secondary organic aerosol formation from
614 reactions of n-alkanes with OH radicals in the presence of NOx, Environmental Science & Technology,
615 39, 9229-9236, 10.1021/es051447g, 2005.

Lim, Y. B., and Ziemann, P. J.: Effects of Molecular Structure on Aerosol Yields from OH Radical-Initiated Reactions of Linear, Branched, and Cyclic Alkanes in the Presence of NOx, Environmental Science & Technology, 43, 2328-2334, 10.1021/es803389s, 2009.

Loza, C. L., Craven, J. S., Yee, L. D., Coggon, M. M., Schwantes, R. H., Shiraiwa, M., Zhang, X., Schilling, K. A., Ng, N. L., Canagaratna, M. R., Ziemann, P. J., Flagan, R. C., and Seinfeld, J. H.: Secondary organic aerosol yields of 12-carbon alkanes, Atmospheric Chemistry and Physics, 14, 1423-1439, 10.5194/acp-14-1423-2014, 2014.

Ma, P. K., Zhao, Y., Robinson, A. L., Worton, D. R., Goldstein, A. H., Ortega, A. M., Jimenez, J. L., Zotter, P., Prevot, A. S. H., Szidat, S., and Hayes, P. L.: Evaluating the impact of new observational constraints on P-S/IVOC emissions, multi-generation oxidation, and chamber wall losses on SOA modeling for Los Angeles, CA, Atmospheric Chemistry and Physics, 17, 9237-9259, 10.5194/acp-17-9237-2017, 2017.

McDonald, B. C., de Gouw, J. A., Gilman, J. B., Jathar, S. H., Akherati, A., Cappa, C. D., Jimenez, J. L., Lee-Taylor, J., Hayes, P. L., McKeen, S. A., Cui, Y. Y., Kim, S.-W., Gentner, D. R., Isaacman-VanWertz, G., Goldstein, A. H., Harley, R. A., Frost, G. J., Roberts, J. M., Ryerson, T. B., and Trainer, M.: Volatile chemical products emerging as largest petrochemical source of urban organic emissions, Science, 359, 760-764, 10.1126/science.aaq0524, 2018.

Mikoviny, T., Kaser, L., and Wisthaler, A.: Development and characterization of a High-Temperature Proton-Transfer-Reaction Mass Spectrometer (HT-PTR-MS), Atmospheric Measurement Techniques Discussions, 3, 185-202, 2010.

Ng, N. L., Kroll, J. H., Chan, A. W. H., Chhabra, P. S., Flagan, R. C., and Seinfeld, J. H.: Secondary organic aerosol formation from m-xylene, toluene, and benzene, Atmospheric Chemistry and Physics, 7, 3909-3922, DOI 10.5194/acp-7-3909-2007, 2007.

Pandis, S. N., Paulson, S. E., Seinfeld, J. H., and Flagan, R. C.: Aerosol formation in the photooxidation of isoprene and β-pinene, Atmospheric Environment. Part A. General Topics, 25, 997-1008, https://doi.org/10.1016/0960-1686(91)90141-S, 1991.

642 Presto, A. A., Miracolo, M. A., Donahue, N. M., and Robinson, A. L.: Secondary organic aerosol
643 formation from high-NO(x) photo-oxidation of low volatility precursors: n-alkanes, Environ Sci
644 Technol, 44, 2029-2034, 10.1021/es903712r, 2010a.
645 Presto, A. A., Miracolo, M. A., Donahue, N. M., and Robinson, A. L.: Secondary Organic Aerosol
646 Formation from High-NOx Photo-Oxidation of Low Volatility Precursors: n-Alkanes, Environmental
647 Science & Technology, 44, 2029-2034, 10.1021/es903712r, 2010b.
648 Pye, H. O. T., and Pouliot, G. A.: Modeling the Role of Alkanes, Polycyclic Aromatic Hydrocarbons,
649 and Their Oligomers in Secondary Organic Aerosol Formation, Environmental Science & Technology,
650 46, 6041-6047, 10.1021/es300409w, 2012.
651 Roberts, J., Marchewka, M., Bertman, S., Goldan, P., Kuster, W., de Gouw, J., warneke, C., Williams,
652 E., Lerner, B., Murphy, P., Apel, E., and Fehsenfeld, F.: Analysis of the isoprene chemistry observed
653 during the New England Air Quality Study (NEAQS) 2002 Intensive Experiment, Journal of
654 Geophysical Research-Atmospheres, 111, D23S12, 10.1029/2006JD007570, 2006.
655 Robinson, A. L., Donahue, N. M., Shrivastava, M. K., Weitkamp, E. A., Sage, A. M., Grieshop, A. P.,
656 Lane, T. E., Pierce, J. R., and Pandis, S. N.: Rethinking organic aerosols: Semivolatile emissions and
657 photochemical aging, Science, 315, 1259-1262, 10.1126/science.1133061, 2007.
658 Sangiorgi, G., Ferrero, L., Perrone, M. G., Papa, E., and Bolzacchini, E.: Semivolatile PAH and n-
659 alkane gas/particle partitioning using the dual model: up-to-date coefficients and comparison with
660 experimental data, Environmental Science and Pollution Research, 21, 10163-10173, 10.1007/s11356-
661 014-2902-z, 2014.
662 Stark, H., Yatavelli, R. L. N., Thompson, S. L., Kimmel, J. R., Cubison, M. J., Chhabra, P. S.,
663 Canagaratna, M. R., Jayne, J. T., Worsnop, D. R., and Jimenez, J. L.: Methods to extract molecular and
664 bulk chemical information from series of complex mass spectra with limited mass resolution,
665 International Journal of Mass Spectrometry, 389, 26-38, https://doi.org/10.1016/j.ijms.2015.08.011,
666 2015.
667 Tajuelo, M., Rodriguez, D., Teresa Baeza-Romero, M., Diaz-de-Mera, Y., Aranda, A., and Rodriguez,
668 A.: Secondary organic aerosol formation from styrene photolysis and photooxidation with hydroxyl
669 radicals, Chemosphere, 231, 276-286, 10.1016/j.chemosphere.2019.05.136, 2019.

Takekawa, H., Minoura, H., and Yamazaki, S.: Temperature dependence of secondary organic aerosol formation by photo-oxidation of hydrocarbons, Atmospheric Environment, 37, 3413-3424, https://doi.org/10.1016/S1352-2310(03)00359-5, 2003.

Timonen, H., Cubison, M., Aurela, M., Brus, D., Lihavainen, H., Hillamo, R., Canagaratna, M., Nekat, B., Weller, R., Worsnop, D., and Saarikoski, S.: Applications and limitations of constrained high-resolution peak fitting on low resolving power mass spectra from the ToF-ACSM, Atmos. Meas. Tech., 9, 3263-3281, 10.5194/amt-9-3263-2016, 2016.

Tkacik, D. S., Presto, A. A., Donahue, N. M., and Robinson, A. L.: Secondary Organic Aerosol Formation from Intermediate-Volatility Organic Compounds: Cyclic, Linear, and Branched Alkanes, Environmental Science & Technology, 46, 8773-8781, 10.1021/es301112c, 2012.

Wu, C., Wang, C., Wang, S., Wang, W., Yuan, B., Qi, J., Wang, B., Wang, H., Wang, C., Song, W., Wang, X., Hu, W., Lou, S., Ye, C., Peng, Y., Wang, Z., Huangfu, Y., Xie, Y., Zhu, M., Zheng, J., Wang, X., Jiang, B., Zhang, Z., and Shao, M.: Measurement Report: important contributions of oxygenated compounds to emissions and chemistry of VOCs in urban air, Atmos. Chem. Phys. Discuss., 2020, 1-37, 10.5194/acp-2020-152, 2020.

Wu, L., Wang, X., Lu, S., Shao, M., and Ling, Z.: Emission inventory of semi-volatile and intermediate-volatility organic compounds and their effects on secondary organic aerosol over the Pearl River Delta region, Atmospheric Chemistry and Physics, 19, 8141-8161, 10.5194/acp-19-8141-2019, 2019.

Xie, M., Hannigan, M. P., and Barsanti, K. C.: Gas/particle partitioning of n-alkanes, PAHs and oxygenated PAHs in urban Denver, Atmospheric Environment, 95, 355-362, https://doi.org/10.1016/j.atmosenv.2014.06.056, 2014.

Yang, W., Li, J., Wang, M., Sun, Y., and Wang, Z.: A Case Study of Investigating Secondary Organic Aerosol Formation Pathways in Beijing using an Observation-based SOA Box Model, Aerosol and Air Quality Research, 18, 1606-1616, 10.4209/aaqr.2017.10.0415, 2018.

Yuan, B., Chen, W. T., Shao, M., Wang, M., Lu, S. H., Wang, B., Liu, Y., Chang, C. C., and Wang, B. G.: Measurements of ambient hydrocarbons and carbonyls in the Pearl River Delta (PRD), China, Atmospheric Research, 116, 93-104, 10.1016/j.atmosres.2012.03.006, 2012.

Yuan, B., Hu, W. W., Shao, M., Wang, M., Chen, W. T., Lu, S. H., Zeng, L. M., and Hu, M.: VOC emissions, evolutions and contributions to SOA formation at a receptor site in eastern China, Atmospheric Chemistry and Physics, 13, 8815-8832, 10.5194/acp-13-8815-2013, 2013.

Yuan, B., Koss, A. R., Warneke, C., Coggon, M., Sekimoto, K., and de Gouw, J. A.: Proton-Transfer-Reaction Mass Spectrometry: Applications in Atmospheric Sciences, Chem Rev, 117, 13187-13229, 10.1021/acs.chemrev.7b00325, 2017a.

Yuan, B., Koss, A. R., Warneke, C., Coggon, M., Sekimoto, K., and de Gouw, J. A.: Proton-Transfer-Reaction Mass Spectrometry: Applications in Atmospheric Sciences, Chemical Reviews, 117, 13187-13229, 10.1021/acs.chemrev.7b00325, 2017b.

Zhao, Y., Kreisberg, N. M., Worton, D. R., Teng, A. P., Hering, S. V., and Goldstein, A. H.: Development of anIn SituThermal Desorption Gas Chromatography Instrument for Quantifying Atmospheric Semi-Volatile Organic Compounds, Aerosol Science and Technology, 47, 258-266, 10.1080/02786826.2012.747673, 2013.

Zhao, Y., Hennigan, C. J., May, A. A., Tkacik, D. S., de Gouw, J. A., Gilman, J. B., Kuster, W. C., Borbon, A., and Robinson, A. L.: Intermediate-Volatility Organic Compounds: A Large Source of Secondary Organic Aerosol, Environmental Science & Technology, 48, 13743-13750, 10.1021/es5035188, 2014a.

Zhao, Y., Hennigan, C. J., May, A. A., Tkacik, D. S., de Gouw, J. A., Gilman, J. B., Kuster, W. C., Borbon, A., and Robinson, A. L.: Intermediate-volatility organic compounds: a large source of secondary organic aerosol, Environ Sci Technol, 48, 13743-13750, 10.1021/es5035188, 2014b.

Zhao, Y., Nguyen, N. T., Presto, A. A., Hennigan, C. J., May, A. A., and Robinson, A. L.: Intermediate Volatility Organic Compound Emissions from On-Road Diesel Vehicles: Chemical Composition, Emission Factors, and Estimated Secondary Organic Aerosol Production, Environ Sci Technol, 49, 11516-11526, 10.1021/acs.est.5b02841, 2015.

Zhao, Y., Nguyen, N. T., Presto, A. A., Hennigan, C. J., May, A. A., and Robinson, A. L.: Intermediate Volatility Organic Compound Emissions from On-Road Gasoline Vehicles and Small Off-Road Gasoline Engines, Environ Sci Technol, 50, 4554-4563, 10.1021/acs.est.5b06247, 2016.

724 Zhu, J., Penner, J. E., Lin, G., Zhou, C., Xu, L., and Zhuang, B.: Mechanism of SOA formation
725 determines magnitude of radiative effects, Proceedings of the National Academy of Sciences of the
726 United States of America, 114, 12685-12690, 10.1073/pnas.1712273114, 2017.

727

728 **Table 1**. Fractions of product ions (m-1) ions in mass spectra, sensitivities, response time

729 and detection limits of higher alkanes in NO^+ PTR-ToF-MS.

Compounds	Ions	Fractions of	Sensitivities	Response time	Detection limit for	Detection limit for
n-Octane	$C_8H_{17}^+$	24	104.6	9.0	3.5	1.3
n-Nonane	$C_9H_{19}^+$	32	106.3	13.3	3.2	1.2
n- *n*-Decane	$C_{10}H_{21}^+$	39	120.9	14.1	3.5	1.3
n-Undecane	$C_{11}H_{23}^+$	44	140.9	4.2	3.3	1.2
n-Dodecane	$C_{12}H_{25}^+$	62	156.3	2.0	2.4	0.9
n-Tridecane	$C_{13}H_{27}^+$	61	186.6	3.4	2.1	0.8
n-Tetradecane	$C_{14}H_{29}^+$	64	220.7	18.2	1.9	0.7
n-Pentadecane	$C_{15}H_{31}^+$	84	205.5	7.6	1.7	0.6
n-Hexadecane	$C_{16}H_{33}^+$	95	/	20.0	1.6	0.6
n-Heptadecane	$C_{17}H_{35}^+$	82	/	30.7	1.8	0.7
n-Octadecane	$C_{18}H_{37}^+$	90	/	34.9	1.8	0.7
n-Nonadecane	$C_{19}H_{39}^+$	71	/	28.8	1.2	0.4
n-Eicosane	$C_{20}H_{41}^+$	86	/	53.4	1.9	0.7
n-Heneicosane	$C_{21}H_{43}^+$	/	/	115.9	2.0	0.7

730

731

732 **Table 2.** Mean concentrations of alkanes (C8-C21) in different sites worldwide.

Compounds	Formula	PRD, China[a] (ppt)	PRD, China[b] (ppt)	NCP, China[a] (ppt)	Paris, France[c] (ppt)	Pasadena, US[d] (ppt)
Octane	C_8H_{18}	482±488	50±49	412±270	/	/
Nonane	C_9H_{20}	208±186	43±32	252±162	14±13	/
Decane	$C_{10}H_{22}$	174±199	29±28	224±147	24±22	/
Undecane	$C_{11}H_{24}$	129±138	21±17	170±119	19±16	/
Dodecane	$C_{12}H_{26}$	122±120	/	129±86	22±21	8±1
Tridecane	$C_{13}H_{28}$	66±60	/	89±59	13±12	6±1
Tetradecane	$C_{14}H_{30}$	50±47	/	57±39	27±23	9±2
Pentadecane	$C_{15}H_{32}$	45±42	/	46±33	23±18	5±0.8
Hexadecane	$C_{16}H_{34}$	36±33	/	32±24	22±19	4±1
Heptadecane	$C_{17}H_{36}$	21±20	/	18±14	/	3±0.4
Octadecane	$C_{18}H_{38}$	13±14	/	11±9	/	1.6±0.5
Nonadecane	$C_{19}H_{40}$	5±9	/	4±7	/	0.7±0.2
Eicosane	$C_{20}H_{42}$	0.7±4	/	3±6	/	0.24±0.08
Heneicosane	$C_{21}H_{44}$	0.5±5	/	2±5	/	0.15±0.1

733 [a]: alkanes measured with NO^+ PTR-ToF-MS; [b]: *n*-alkanes measured with GC-MS; [c]: *n*-alkanes from Ait-Helal

734 et al. (2014); [d]: *n*-alkanes from Zhao et al. (2014a).

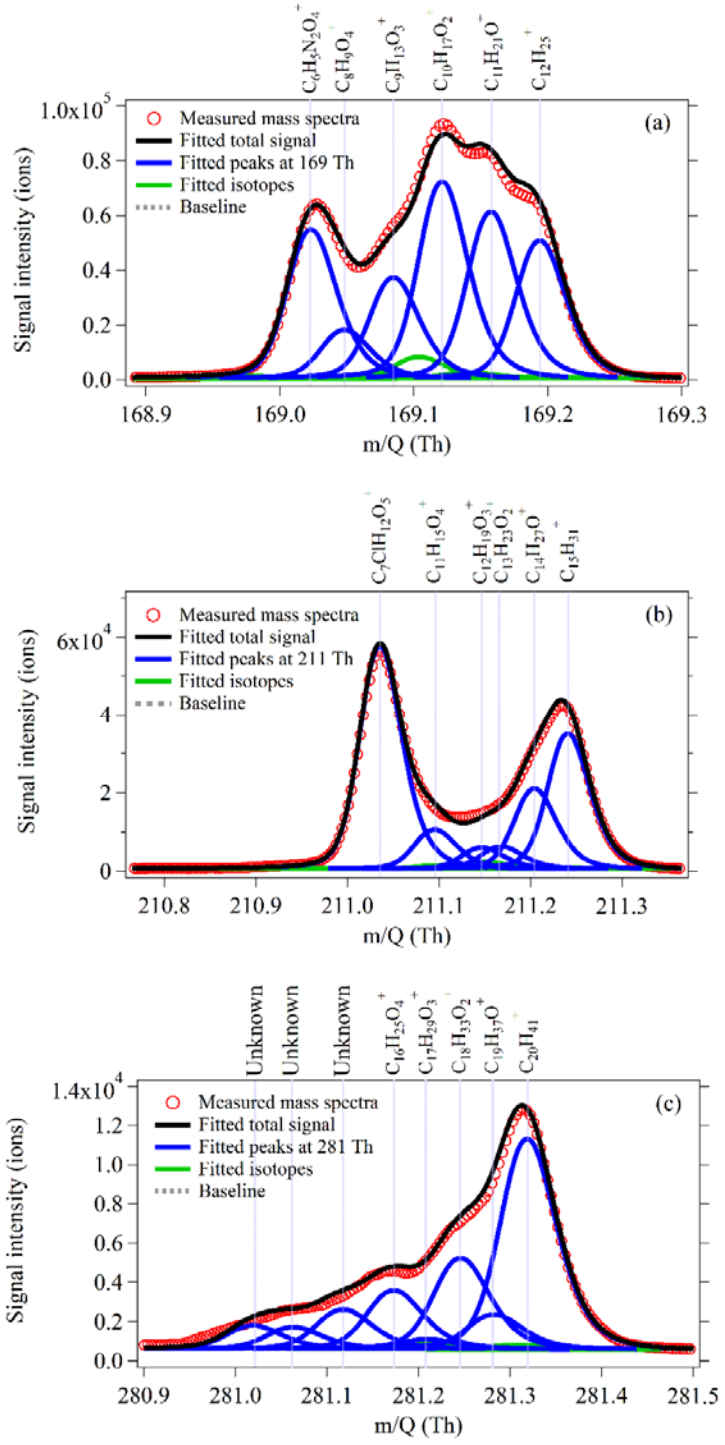

735

736 **Figure 1.** High-resolution (HR) peak-fitting to the averaged mass spectra on a typical day (12
737 October 2018) for m/z 169 **(a)**, m/z 211 **(b)** and m/z 281 **(c)**, at which masses produced by
738 dodecane ($C_{12}H_{25}^+$), pentadecane ($C_{15}H_{31}^+$) and eicosane ($C_{20}H_{41}^+$) produced in NO^+ PTR-ToF-
739 MS.

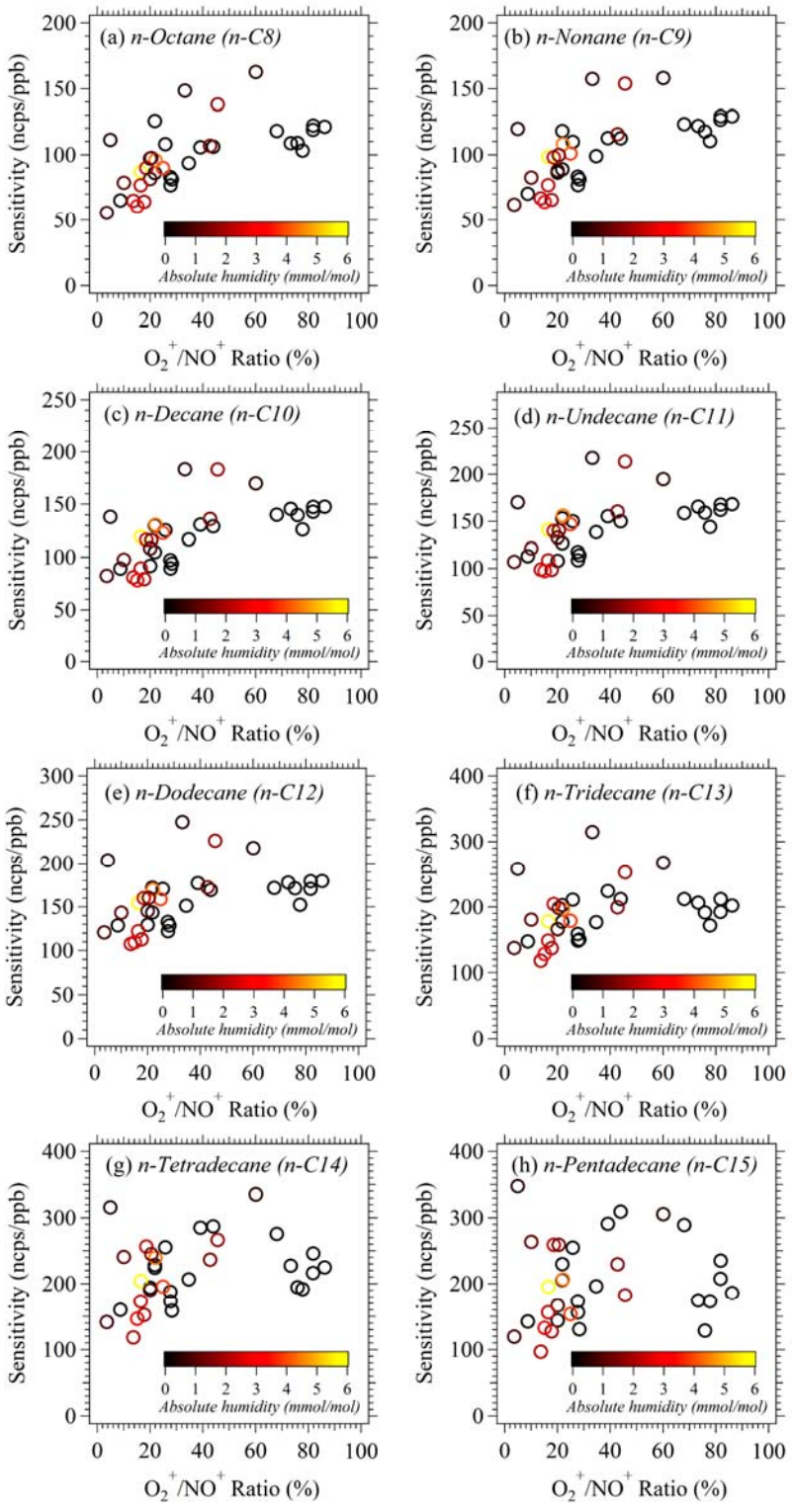

740

741 **Figure 2.** The relationship of sensitivities of *n*-alkanes (C8-C15) versus O_2^+/NO^+ ratios during
742 the NCP campaign. The data points are color-coded using absolute humidity during the
743 calibration.

744 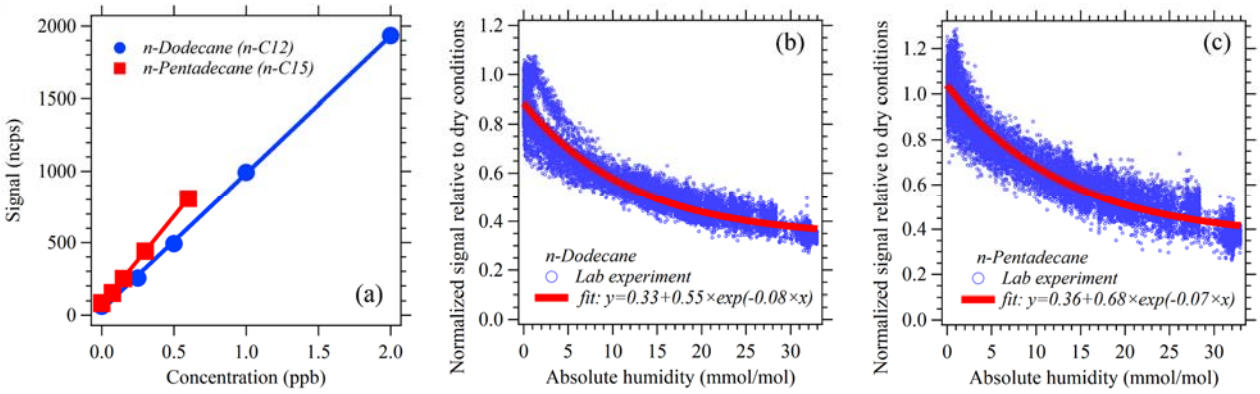

745 **Figure 3**. **(a)** Calibrations of *n*-Dodecane and *n*-Pentadecane under dry conditions; **(b)**

746 Humidity dependence of *n*-Dodecane. **(c)** Humidity dependence of *n*-Pentadecane.

747

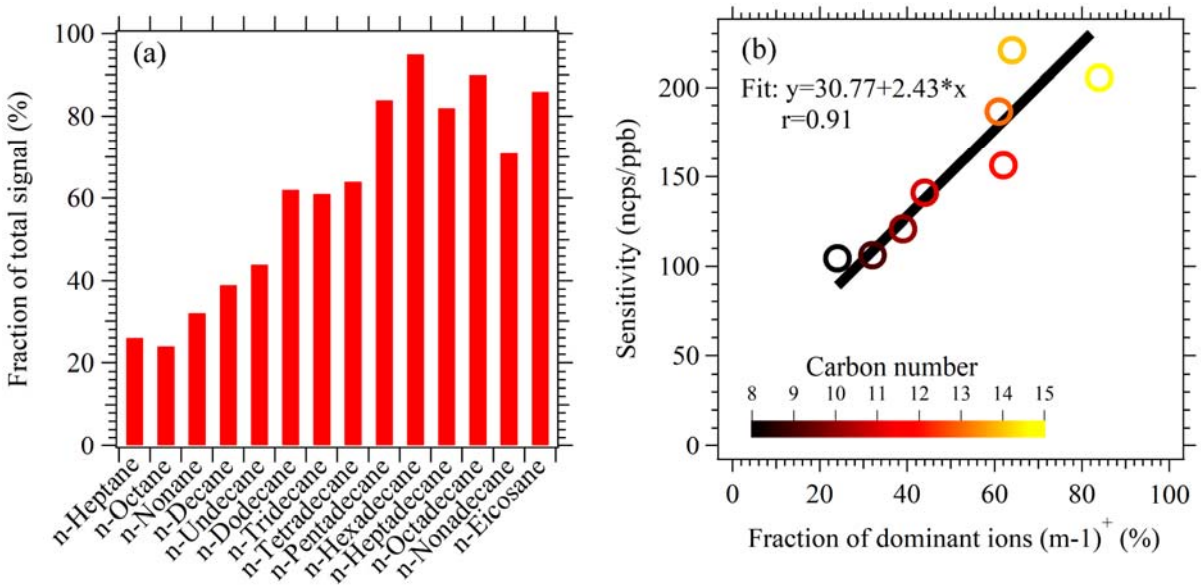

748

749 **Figure 4. (a)** The fractions of product ions (m-1) from hydride abstraction of C8-C20 *n*-alkanes

750 in NO^+ PTR-ToF-MS. **(b)** Scatterplot of sensitivities under dry conditions versus the fractions

751 of hydride abstraction ions for C8-C15 *n*-alkanes.

752

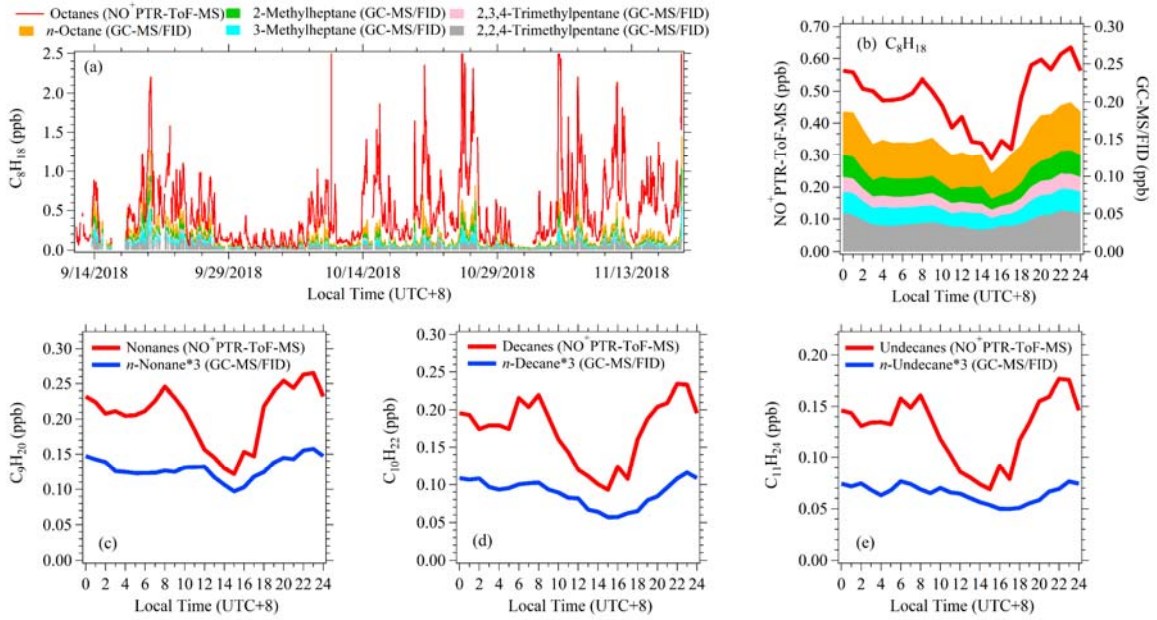

753

754 **Figure 5.** Comparisons of times series and diurnal variations of alkanes measured by NO^+
755 PTR-ToF-MS and GC-MS/FID in PRD. **(a)** Time series of C8 alkanes measured by NO^+ PTR-
756 ToF-MS, C8 *n*-alkane and four branched isomers measured by GC-MS/FID. **(b)** Diurnal
757 variations of C8 alkanes. **(c-e)** Diurnal variations of C9-C11 alkanes with NO^+ PTR-ToF-MS
758 and C9-C11 *n*-alkanes with GC-MS/FID.

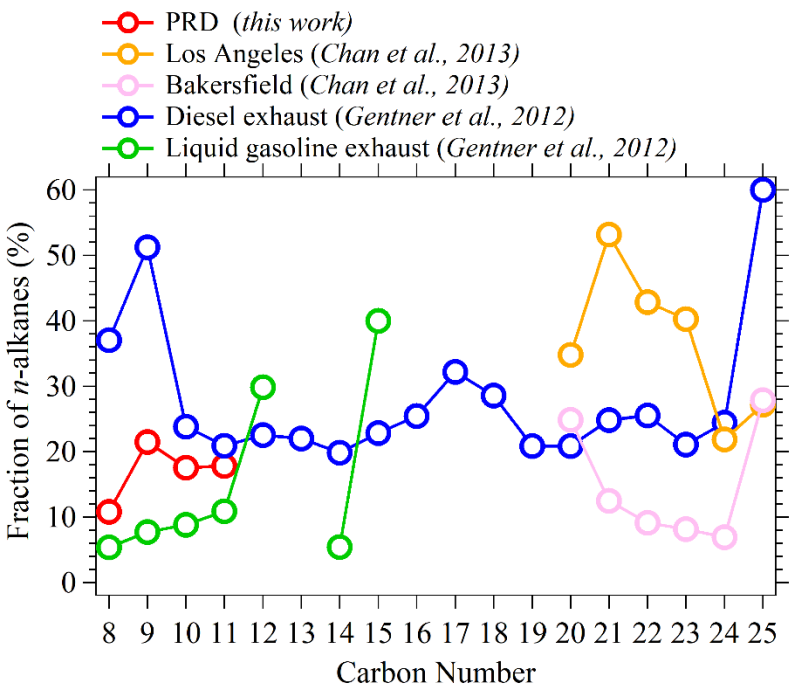

759

760 **Figure 6.** Fractions of *n*-alkanes in higher alkanes with same formulas derived from this
761 study, ambient air in Los Angeles, Bakersfield and in vehicle exhausts (Chan et al.,
762 2013;Gentner et al., 2012).

763

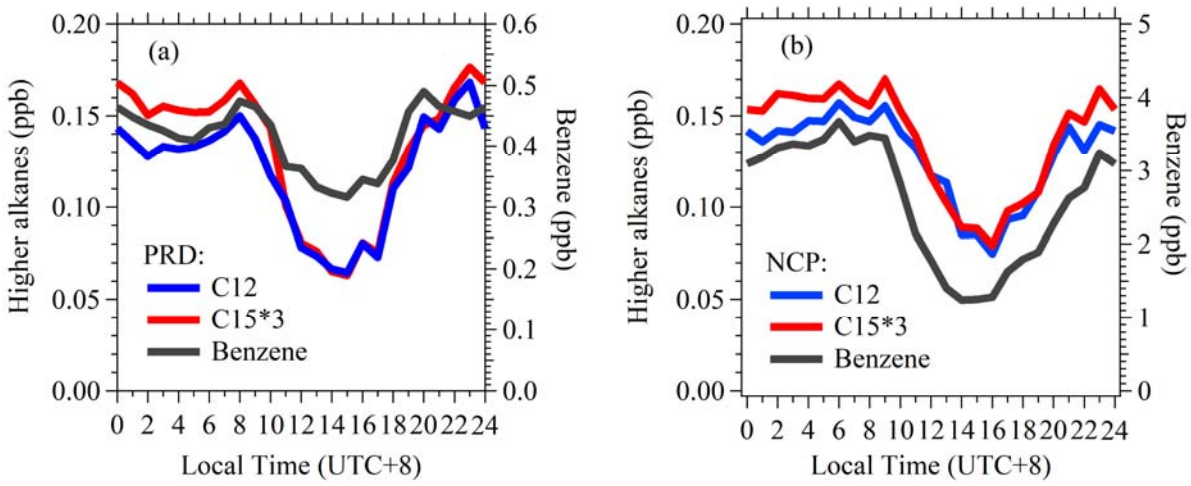

764

765 **Figure 7.** Diurnal variations of C12 alkanes, C15 alkanes and benzene in PRD **(a)** and NCP

766 **(b)**.

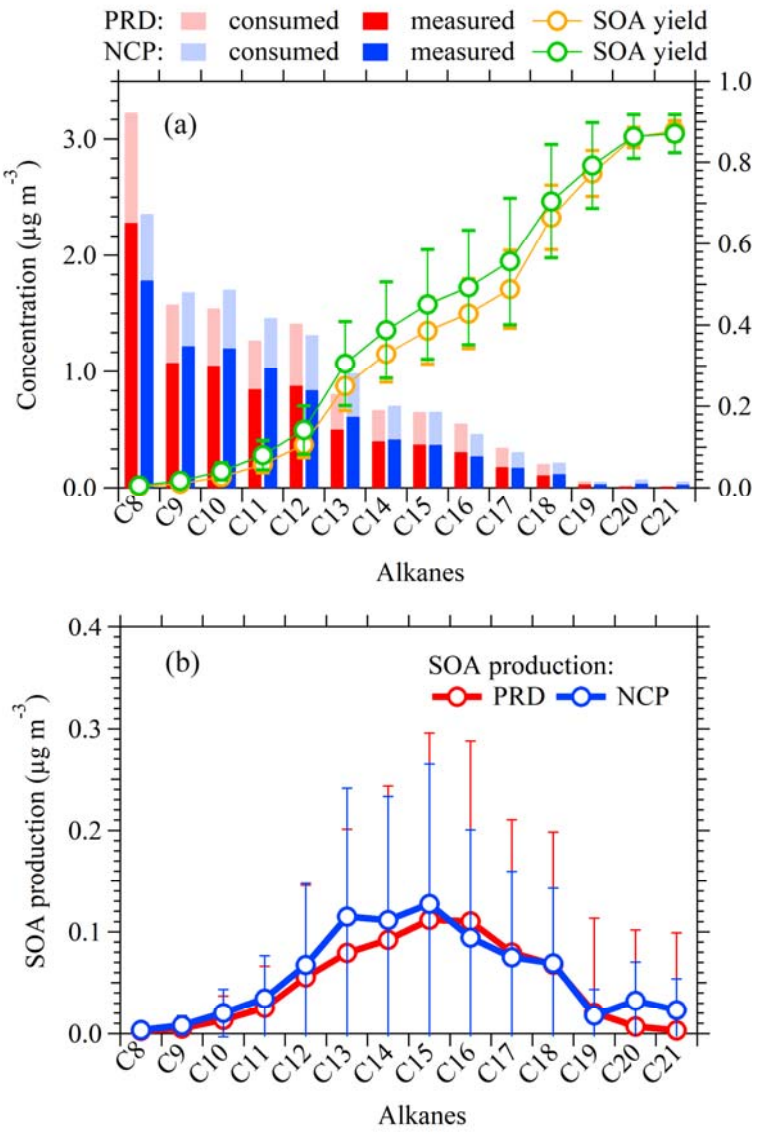

767

768 **Figure 8. (a)** Measured concentrations by NO^+ PTR-ToF-MS, calculated consumed
769 concentrations and average SOA yields for C8-C21 alkanes in PRD and NCP. The error bars
770 represent standard deviations (1δ) over the averaging period of calculated SOA yields. **(b)**
771 Calculated average SOA productions for C8-C21 alkanes in PRD and NCP. The error bars
772 represent standard deviations (1δ) over the averaging period of calculated SOA production.

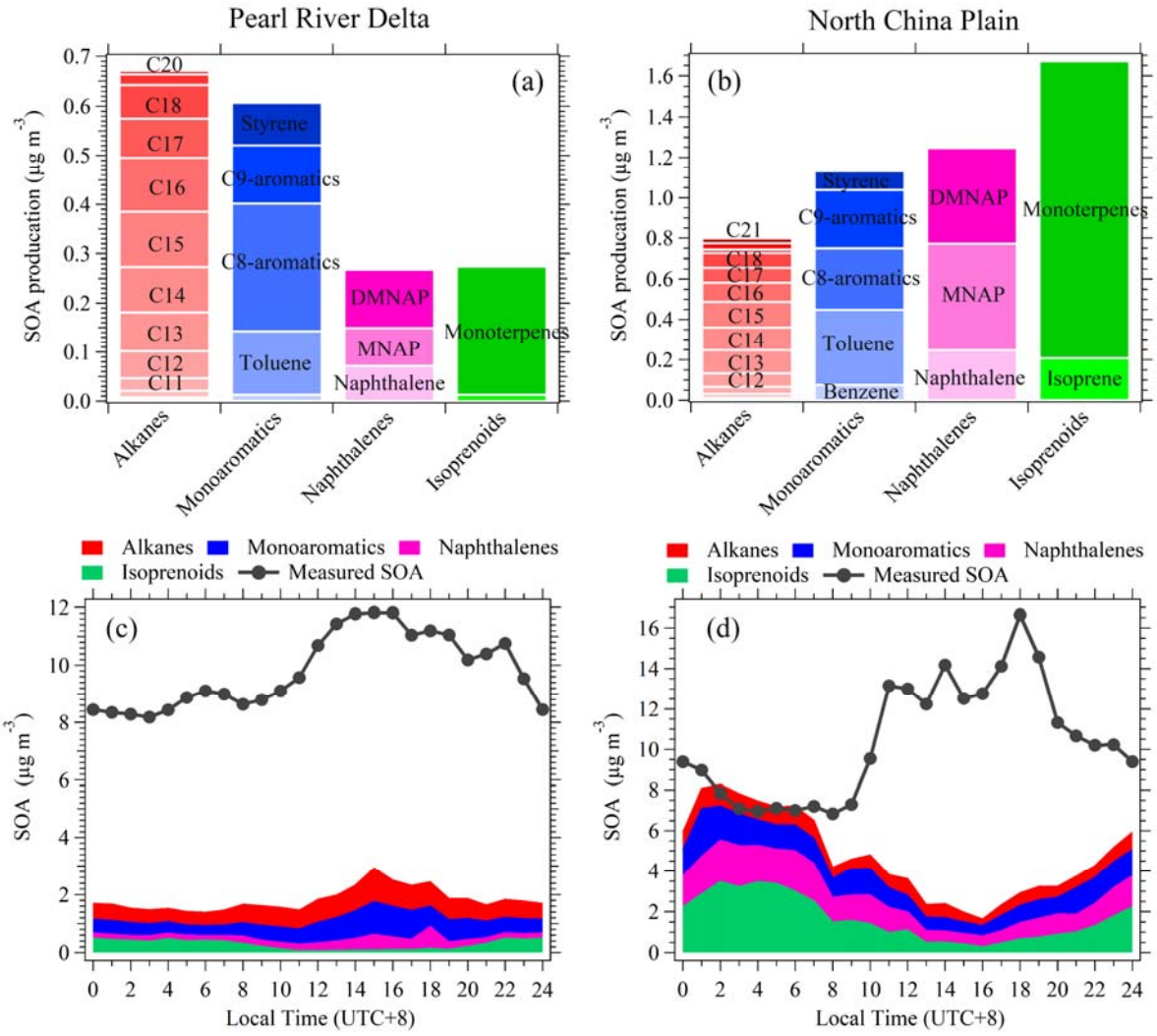

Figure 9. The mean concentrations of SOA produced from higher alkanes (C8-C21 alkanes), monoaromatics (benzene, toluene, C8 aromatics, C9 aromatics and styrene), naphthalenes (naphthalene, methylnaphthalenes, dimethylnaphthalenes) and isoprenoids (isoprene and monoterpenes) in PRD **(a)** and NCP **(b)**. Diurnal variations of SOA production from higher alkanes, monoaromatics, naphthalenes and isoprenoids as well as the measured SOA concentrations in PRD **(c)** and NCP **(d)**.